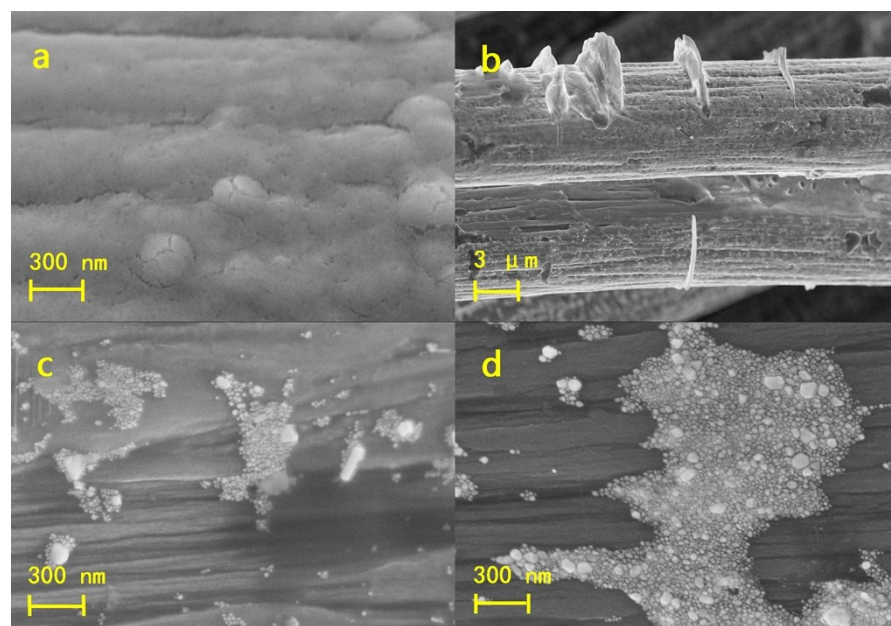


Supplementary information:

## Uncover the role of Ag in layer-alternating Ni<sub>3</sub>S<sub>2</sub>/Ag/Ni<sub>3</sub>S<sub>2</sub> as electrocatalyst with enhanced OER performance

Rui Guo<sup>1,2,3</sup>, Yan He<sup>1,3,\*</sup>, Renchao Wang<sup>1,3</sup>, Junhua You<sup>4</sup>, Hongji Lin<sup>5</sup>, Chiente Chen<sup>5</sup>, Tingshan Chan<sup>5</sup>, Xuanwen Liu<sup>1,3,\*</sup>, Zhiwei Hu<sup>6,\*</sup>



**Fig. S1.** SEM images of Ag samples by electrodeposition for (a) 2 s, (b) 4 s, (c) 6 s, (d) 8 s.

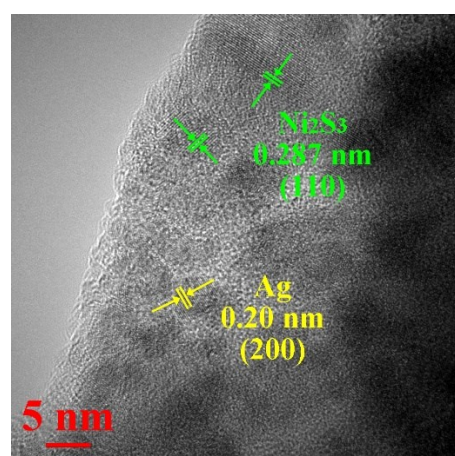


**Fig. S2.** The HRTEM images of N1A1.

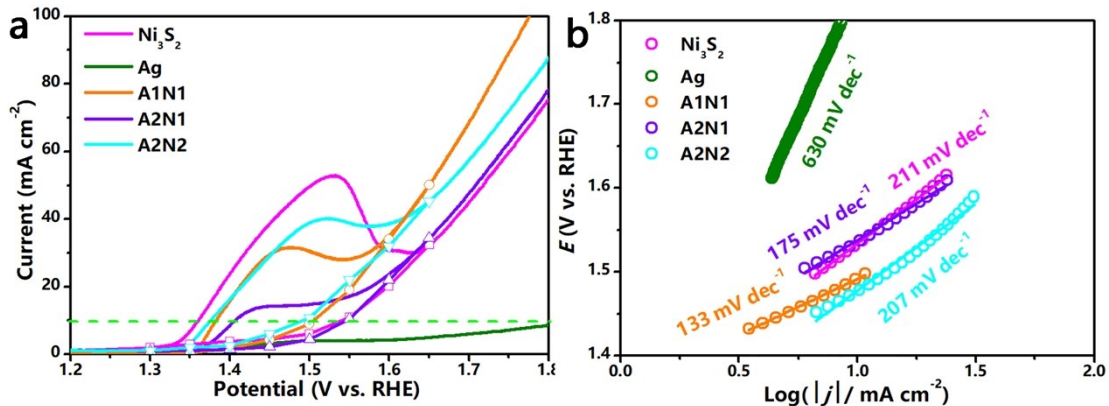


**Fig. S3.** (a) The OER polarization curves and (b) Tafel plots of Ni<sub>3</sub>S<sub>2</sub>, Ag, A1N1, A2N1, and A2N2

**Table S1.** Comparision of the OER performance of N2A1 with Ni<sub>3</sub>S<sub>2</sub> electrocatalysts in alkaline electrolyte.

Catalysts	$\eta_{10}$ (mV)	Tafel Slope <sup>a</sup> (mV dec <sup>-1</sup> )	Electrolyte	Ref.
Ni <sub>3</sub> S <sub>2</sub> nanoporous thin films	319 @ 20 mA cm <sup>-2</sup>	101.2	1.0 M KOH	S1
Ni <sub>3</sub> S <sub>2</sub> /VS <sub>2</sub>	227	59.9	1.0 M NaOH	S2
Fe-doped Ni <sub>3</sub> S <sub>2</sub> particles film	253 @ 100 mA cm <sup>-2</sup>	65.5	1.0 M KOH	S3
Ni <sub>3</sub> S <sub>2</sub> nanorods/NF	157	153	1.0 M KOH	S4
Fe <sub>17.5%</sub> -Ni <sub>3</sub> S <sub>2</sub> /NF	214	42	1.0 M KOH	S5
Ni <sub>3</sub> S <sub>2</sub> /NF-2	425 @ 100 mA cm <sup>-2</sup>	-	1.0 M KOH	S6
Co <sub>3</sub> O <sub>4</sub> @Ni <sub>3</sub> S <sub>2</sub> /NF	260 @ 20 mA cm <sup>-2</sup>	121.7	1.0 M KOH	S7
CdS/Ni <sub>3</sub> S <sub>2</sub> /PNF	151	174	1.0 M KOH	S8
Ag/Ni <sub>3</sub> S <sub>2</sub> (N2A1)	187	118	1.0 M KOH	This work

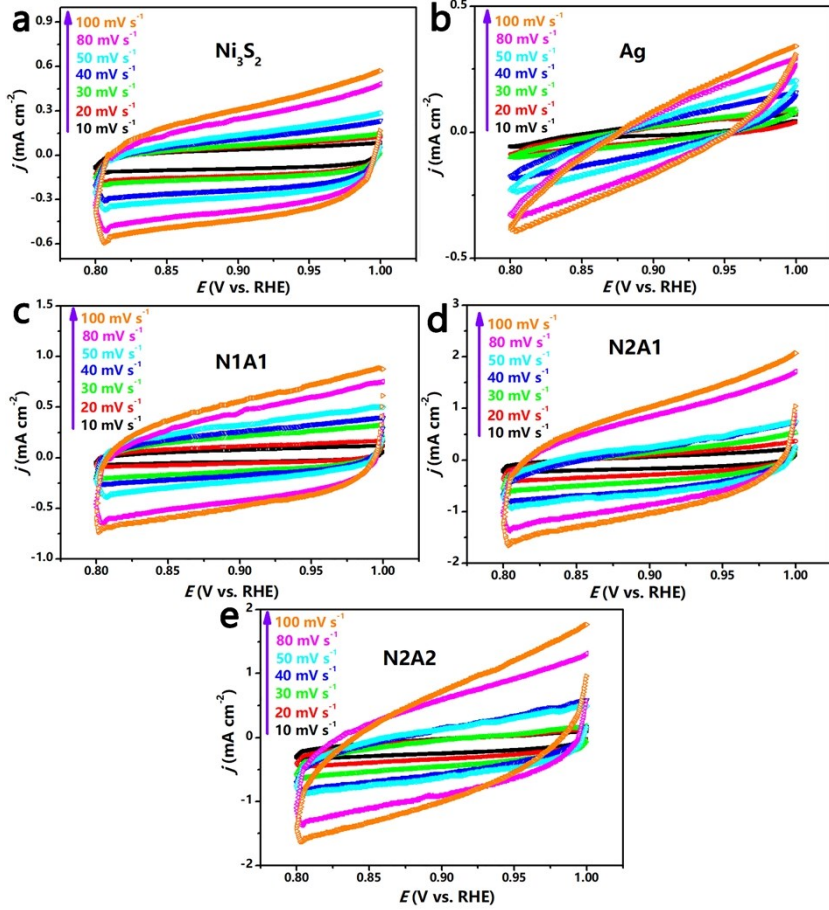


**Fig. S4.** Cyclic voltammogram curves of  $\text{Ni}_3\text{S}_2$  (a), Ag (b), N1A1 (c), N2A1 (d), and N2A2 (d)

measured in the range of 0.8 ~ 1.0 V vs. RHE at different scan rates: 10, 20, 30, 40, 50, 80, and 100  $\text{mV s}^{-1}$ .

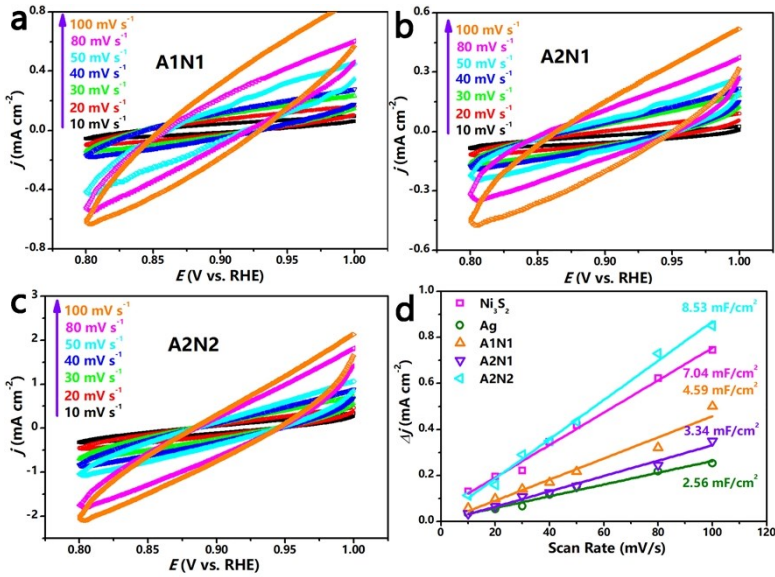


**Fig. S5.** Cyclic voltammogram curves of A1N1 (a), A2N1 (b), and A2N2 (c) measured in the range of 0.8 ~ 1.0 V vs. RHE at different scan rates: 10, 20, 30, 40, 50, 80, and 100  $\text{mV s}^{-1}$ . (d)

Double layer capacitance (Cdl) of as-prepared electrocatalysts.

**Table S2.** Electrocatalytic performances of different samples

Sample	OER		$R_{ct}/\Omega$	$W/\Omega$
	$\eta_j @ 10 \text{ mA cm}^{-2}$	Tafel slope (mV dec $^{-1}$ )		
Ag	-	630	6.25	53.31
Ni <sub>3</sub> S <sub>2</sub>	308	211	0.56	3.42
N1A1	289	190	0.41	2.14
N2A1	187	118	0.19	1.62
N2A2	233	154	0.50	1.61

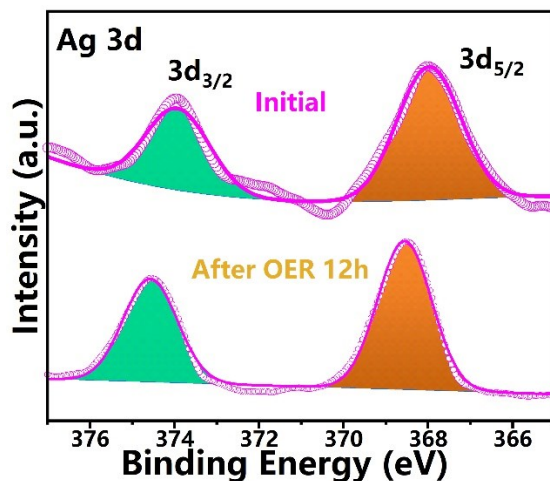


**Fig. S6.** High resolution XPS spectra of Ag 3d before and after OER for 12 h.

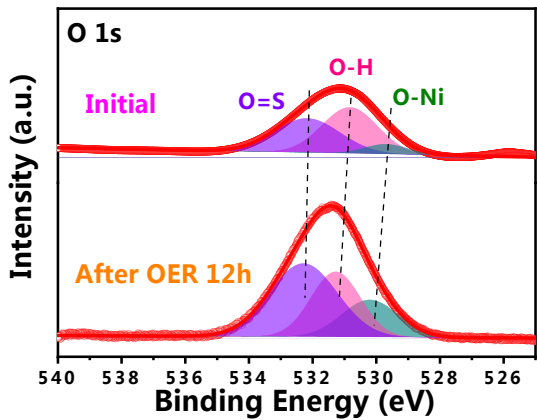


**Fig. S7.** High resolution XPS spectrums of O 1S of N2A1 before and after OER for 12 h.

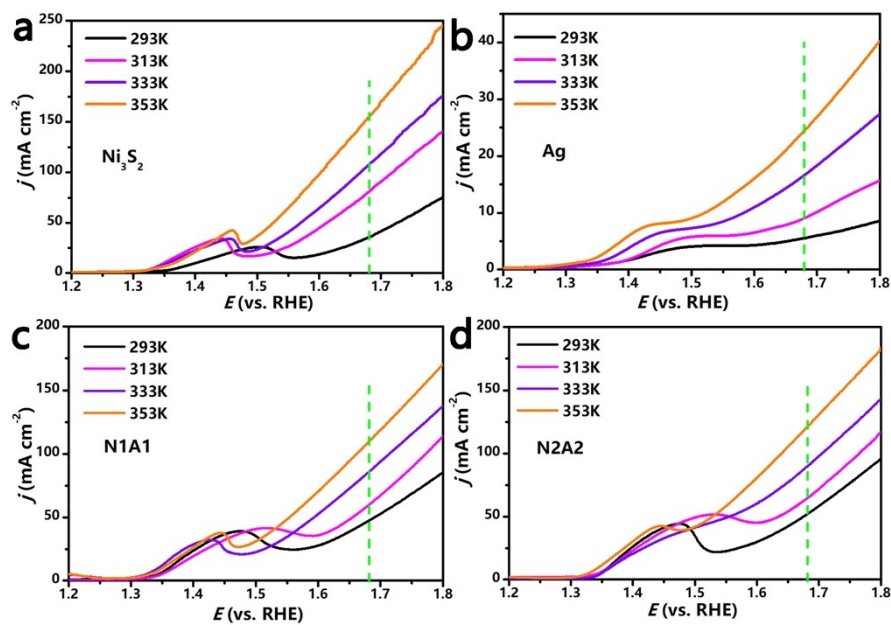


**Fig. S8.** LSV curves of  $\text{Ni}_3\text{S}_2$  (a), Ag (b), N1A1 (c), and N2A2 (d) at a scan rate of  $5 \text{ mV s}^{-1}$  in  $1.0 \text{ M KOH}$  towards OER as the temperature rose from 293 to 353 K.

## Reference

- S1 J. Dong, F. Zhang, Y. Yang, Y. Zhang, H. He, X. Huang, X. Fan and X. Zhang, (003)-Facet-exposed Ni<sub>3</sub>S<sub>2</sub> nanoporous thin films on nickel foil for efficient water splitting, *Appl. Catal. B*, 2019, **243**, 693-702.
- S2 X. Zhong, J. Tang, J. Wang, M. Shao, J. Chai, S. Wang, M. Yang, Y. Yang, N. Wang, S. Wang, B. Xu and H. Pan, 3D heterostructured pure and N-Doped Ni<sub>3</sub>S<sub>2</sub>/VS<sub>2</sub> nanosheets for high efficient overall water splitting, *Electrochim. Acta*, 2018, **269**, 55-61.
- S3 N. Cheng, Q. Liu, A. M. Asiri, W. Xing and X. Sun, A Fe-doped Ni<sub>3</sub>S<sub>2</sub> particle film as a high-efficiency robust oxygen evolution electrode with very high current density, *J. Mater. Chem. A*, 2015, **3**, 23207-23212.
- S4 W. Zhou, X. Wu, X. Cao, X. Huang, C. Tan, J. Tian, H. Liu, J. Wang and H. Zhang, Ni<sub>3</sub>S<sub>2</sub> nanorods/Ni foam composite electrode with low overpotential for electrocatalytic oxygen evolution, *Energy Environ. Sci.*, 2013, **6**, 2921-2924.
- S5 G. Zhang, Y. Feng, W. Lu, D. He, C. Wang, Y. Li, X. Wang and F. Cao, Enhanced Catalysis of Electrochemical Overall Water Splitting in Alkaline Media by Fe Doping in Ni<sub>3</sub>S<sub>2</sub> Nanosheet Arrays, *ACS Catal.*, 2018, **8**, 5431-5441.
- S6 G. Liu, Z. Sun, X. Zhang, H. Wang, G. Wang, X. Wu, H. Zhang and H. Zhao, Vapor-phase hydrothermal transformation of a nanosheet array structure Ni(OH)<sub>2</sub> into ultrathin Ni<sub>3</sub>S<sub>2</sub> nanosheets on nickel foam for high-efficiency overall water splitting, *J. Mater. Chem. A*, 2018, **6**, 19201-19209.
- S7 Y. Gong, Z. Xu, H. Pan, Y. Lin, Z. Yang and X. Du, Hierarchical Ni<sub>3</sub>S<sub>2</sub> nanosheets coated on Co<sub>3</sub>O<sub>4</sub> nanoneedle arrays on 3D nickel foam as an efficient electrocatalyst for the oxygen evolution reaction, *J. Mater. Chem. A*, 2018, **6**, 5098-5106.
- S8 S. Qu, J. Huang, J. Yu, G. Chen, W. Hu, M. Yin, R. Zhang, S. Chu and C. R. Li, Ni<sub>3</sub>S<sub>2</sub> Nanosheet Flowers Decorated with CdS Quantum Dots as a Highly Active Electrocatalysis Electrode for Synergistic Water Splitting, *ACS Appl. Mater. Interfaces*, 2017, **9**, 29660-29668.